Applications of Sphere Geometry in Canal Surface Design

Christoph Mäurer

Abstract. Classical models of sphere geometry facilitate an efficient description of canal surfaces. Using the cyclographic model of Laguerre geometry, an elementary characterization of continuity, bisectors, control point-, control sphere- and implicit representations of canal surfaces is presented. In addition, canal surfaces generated with the aid of Minkowski Pythagorean hodograph curves are investigated.

§1. Introduction

A canal surface C in $\mathbb{R}^3$ is defined as the envelope surface of a moving sphere $S(t)$ with center $\boldsymbol{m}(t) := (m_1(t), m_2(t), m_3(t))$ and radius function $r(t)$. The moving sphere can be described with the implicit equation

$$F(\boldsymbol{x}, t) = \|\boldsymbol{x} - \boldsymbol{m}(t)\|^2 - r^2(t) = 0. \tag{1}$$

The envelope condition

$$\frac{\partial F}{\partial t} = [\boldsymbol{x} - \boldsymbol{m}(t)] \cdot \dot{\boldsymbol{m}} + r(t)\dot{r}(t) = 0 \tag{2}$$

describes a moving plane, which intersects $S(t)$ in the characteristic circles of the canal surface. It is a natural approach to use models of classical sphere geometry to study canal surfaces. Well-known models have been investigated in Möbius geometry, Laguerre geometry and Lie geometry. For an overview on sphere geometry, the reader may consult [2]. Papers which handle sphere geometry in the CAGD context are [7,8,10,11,12].

Curve and Surface Design: Saint-Malo 1999
Pierre-Jean Laurent, Paul Sablonnière, and Larry L. Schumaker (eds.), pp. 267–276.

ISBN 0-8265-1356-5.

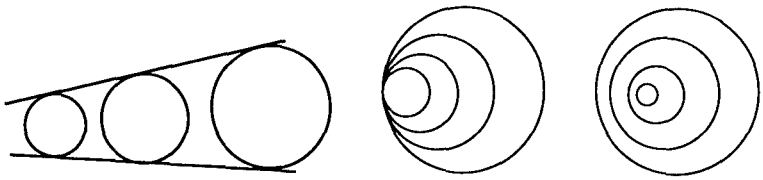

Fig. 1. Hyperbolic, parabolic and elliptic sphere families.

§2. Fundamentals of Laguerre Geometry

In the cyclographic model $\mathbb{R}^{3,1}$ of Laguerre geometry, a sphere S with center $\boldsymbol{m} = (m_1, m_2, m_3)$ and radius r is described as a point $\boldsymbol{s} = (m_1, m_2, m_3, r)^T \in \mathbb{R}^{3,1}$. It is an intuitive model, since the space of points (spheres with vanishing radius) is embedded in the cyclographic model as the hyperplane $x_4 = 0$. The absolute quadric Ω, which reads in homogeneous coordinates $(\underline{x}_i/\underline{x}_0 := x_i)$ as $\Omega : \underline{x}_0 = \underline{x}_1^2 + \underline{x}_2^2 + \underline{x}_3^2 - \underline{x}_4^2 = 0$ plays an important role. It defines a pseudo Euclidean (pe) metric in $\mathbb{R}^{3,1}$ via the scalar product

$$\langle \boldsymbol{a}, \boldsymbol{b} \rangle_{pe} := a_1 b_1 + a_2 b_2 + a_3 b_3 - a_4 b_4. \tag{3}$$

The pe distance $\|\boldsymbol{a} - \boldsymbol{b}\|_{pe} := \sqrt{\langle \boldsymbol{a} - \boldsymbol{b}, \boldsymbol{a} - \boldsymbol{b} \rangle_{pe}}$ of two points $\boldsymbol{a}, \boldsymbol{b} \in \mathbb{R}^{3,1}$ measures the tangential distance of two spheres A, B. First we study the most simple family of spheres described as a line L with direction vector $\boldsymbol{a}$ in $\mathbb{R}^{3,1}$. There are three cases: If $\langle \boldsymbol{a}, \boldsymbol{a} \rangle_{pe} > 0$, then L is called a hyperbolic line corresponding to a family of spheres whose envelope surface is a right circular cone (Fig. 2, left). If $\langle \boldsymbol{a}, \boldsymbol{a} \rangle_{pe} = 0$, then L is called a parabolic or isotropic line belonging to spheres in oriented contact. If $\langle \boldsymbol{a}, \boldsymbol{a} \rangle_{pe} < 0$, then L is called a elliptic line and two arbitrary spheres of such a family do not have a common tangent plane. These three cases of sphere families are plotted in Fig. 1 (but to simplify matters in $\mathbb{R}^2$ instead of $\mathbb{R}^3$). A canal surface is completely determined by the set of its tangent cones. They belong to hyperbolic tangent vectors of a curve $\boldsymbol{c}(t) \in \mathbb{R}^{3,1}$. Vice versa, the set of hyperbolic tangent vectors of $\boldsymbol{c}(t)$ corresponds to the set of tangent cones of a canal surface along the characteristic circles. For elliptic tangent vectors, there does not exist a real tangent cone. Therefore, that case has to be avoided in the specification of canal surfaces. Discrete parameter values t_0 with parabolic tangent vectors ($\|\dot{\boldsymbol{c}}(t_0)\|_{pe} = 0$) are tolerated. At these parameter values, the canal surface is closed (Fig. 2 right).

Corollary 1. *Any real G^1-continuous canal surface C in $\mathbb{R}^3$ can be described as a G^1-continuous curve $\boldsymbol{c}(t) \in \mathbb{R}^{3,1}$ with hyperbolic tangent vectors.*

A Laguerre transformation τ in $\mathbb{R}^{3,1}$ is an affine mapping $\boldsymbol{x} \mapsto \lambda \boldsymbol{A}\boldsymbol{x} + \boldsymbol{b}$, $0 < \lambda \in \mathbb{R}$ which preserves Ω. It turns out that this condition is fulfilled iff $\boldsymbol{A}$ is an orthogonal matrix with respect to the pe metric, i.e.

$$\boldsymbol{A}^T \boldsymbol{E}_{pe} \boldsymbol{A} = \boldsymbol{E}_{pe} := diag(1, 1, 1, -1). \tag{4}$$

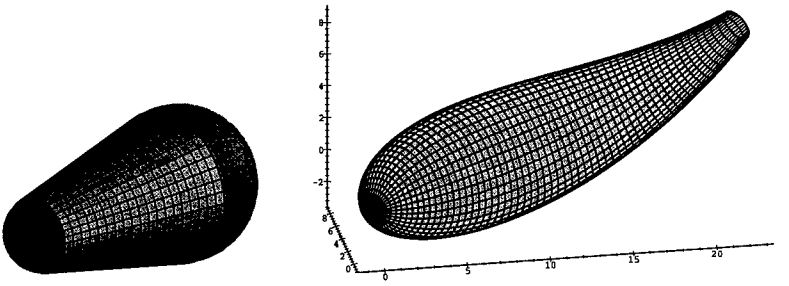

Fig. 2. Left: Tangent cone of two spheres; right: Effect of parabolic tangent vector.

Therefore, Laguerre transformations are pe similarities in $\mathbb{R}^{3,1}$. Since the Euclidean space $\mathbb{R}^3$ is embedded in $\mathbb{R}^{3,1}$, any Euclidean translation or rotation is a Laguerre transformation. The offset operation with offset distance d is described as a translation τ_d in the x_4-direction $(\lambda = 1, \boldsymbol{A} = \boldsymbol{E}, \boldsymbol{b} = (0,0,0,d))$. A further example is the pe rotation around a fixed 2-plane. If the x_2, x_3-plane is fixed, the pe rotation is represented by

$$\tau_r : \begin{pmatrix} x_1 \\ x_4 \end{pmatrix} \mapsto \begin{pmatrix} \cosh\alpha & \sinh\alpha \\ \sinh\alpha & \cosh\alpha \end{pmatrix} \begin{pmatrix} x_1 \\ x_4 \end{pmatrix}. \tag{5}$$

Any Laguerre transformation with $\lambda = 1$ preserves the tangential distance. The following examples show how Laguerre transformations act on simple curves of $\mathbb{R}^{3,1}$.

Example 1. *Consider a straight line $L \in \mathbb{R}^3$. The image line under the offset mapping τ_d describes a cylinder. An additional pe rotation $\tau_r \circ \tau_d(L)$ yields a hyperbolic line corresponding to a right circular cone. Vice versa, any hyperbolic line in $\mathbb{R}^{3,1}$ can be mapped via an appropriate Laguerre transformation to L.*

The line in Example 1 does not change its type under the mappings τ_r and τ_d. Since the sign of $\langle \boldsymbol{a}, \boldsymbol{a} \rangle_{pe}$ is not modified by any Laguerre transformation, we obtain:

Corollary 2. *The type (hyperbolic, parabolic, elliptic) of straight lines in the cyclographic model $\mathbb{R}^{3,1}$ is invariant under Laguerre transformations.*

Example 2. *Consider a Euclidean circle $K \in \mathbb{R}^3$. Its image $\tau_d(K)$ describes a* torus, *and the pe circle $\tau_r \circ \tau_d(K)$ corresponds to a* Dupin cyclide. *Any Dupin cyclide can be interpreted as a circle in $\mathbb{R}^{3,1}$ with respect to the pseudo Euclidean metric. For more details and a proof of this fact, see [7].*

The pe circles might be utilized to describe G^2-continuity between canal surfaces: The osculating pe circle of a curve $\boldsymbol{c}(t) \in \mathbb{R}^{3,1}$ belongs to the osculating cyclide of a canal surface C, which specifies the curvature behaviour of C. A technique to compute osculating circles of space curves in the Euclidean and non-Euclidean space is given in [1].

§3. Isotropic Hypersurfaces

Definition 1. *Let $C \subset \mathbb{R}^3$ be an oriented C^1-continuous canal surface, which belongs to the curve $\boldsymbol{c} \in \mathbb{R}^{3,1}$. The* isotropic hypersurface $\Gamma(\boldsymbol{c}) \subset \mathbb{R}^{3,1}$ *is the union of all points in $\mathbb{R}^{3,1}$ corresponding to all oriented tangent spheres of C.*

For a fixed surface point of C, all oriented tangent spheres are represented as isotropic lines in $\mathbb{R}^{3,1}$. Therefore, $\Gamma(\boldsymbol{c})$ is formed by a two-parametric family of isotropic lines. Applying Corollary 2 to the definition of isotropic hypersurfaces, we obtain:

Proposition 1. *Isotropic hypersurfaces are invariant under Laguerre transformations $\tau(\Gamma(c)) = \Gamma(\tau(c))$.*

The simplest example is the isotropic hypersurface of a sphere S specified by a point $\boldsymbol{s} \in \mathbb{R}^{3,1}$. It is a hypercone $\Gamma(s) = \langle \boldsymbol{x} - \boldsymbol{s}, \boldsymbol{x} - \boldsymbol{s} \rangle_{pe} = 0$. Now consider a canal surface C characterized by a curve $\boldsymbol{c}(t) \in \mathbb{R}^{3,1}$ with hyperbolic tangent vector $\dot{\boldsymbol{c}}(t)$. As shown in [7], its isotropic hypersurface can be achieved in a two-step procedure: First intersect the pe polar plane $\dot{\boldsymbol{c}}_{pe}^{\perp}(t)$ with the absolute quadric Ω (the pe polar plane $\boldsymbol{a}_{pe}^{\perp}$ of a vector $\boldsymbol{a} \in \mathbb{R}^{3,1}$ is defined as $\boldsymbol{a}_{pe}^{\perp} : \boldsymbol{a}^T \boldsymbol{E}_{pe} \boldsymbol{x} = 0$). Then join the resulting family of conics $\boldsymbol{k}(t,s)$ and the curve points $\boldsymbol{c}(t)$ with straight lines. Or as a formula:

$$\Gamma(\boldsymbol{c}) = \cup_t \, \boldsymbol{c}(t) \star \{\dot{\boldsymbol{c}}_{pe}^{\perp}(t) \cap \Omega\},$$

where $A \star B$ denotes all straight lines joining A and B.

Isotropic hypersurfaces have several properties which can be applied in the context of geometric design:

Proposition 2.

1) *The intersection of the isotropic hypersurface $\Gamma(\boldsymbol{c})$ with $\mathbb{R}^3$ generates the canal surface C itself: $\Gamma(\boldsymbol{c}) \cap \mathbb{R}^3 = C$.*
2) *The intersection of $\tau_d(\Gamma(c))$ with $\mathbb{R}^3$ gives the offset surface of C.*
3) *Consider two canal surfaces $C_1, C_2 \in \mathbb{R}^3$ with corresponding curves $\boldsymbol{c}_1(t), \boldsymbol{c}_2(t) \in \mathbb{R}^{3,1}$. These canal surfaces touch each other if $\boldsymbol{c}_2$ is lying on $\Gamma(\boldsymbol{c}_1)$ (resp. if $\boldsymbol{c}_1$ is lying on $\Gamma(\boldsymbol{c}_2)$).*
4) *The bisector surface of C_1 and C_2 is formed by the orthogonal projection of $\{\Gamma(\boldsymbol{c}_1) \cap \Gamma(\boldsymbol{c}_2)\}$ to $\mathbb{R}^3$.*

Proof: *1) The tangent spheres with radius zero of a canal surface are precisely its surface points. They are contained in the hyperplane $\mathbb{R}^3$ of the cyclographic model. 2) follows from the offset property of τ_d and Proposition 1. 3) follows immediately from Definition 1. To prove 4), note that the bisector is characterized as the center of spheres which have oriented contact to C_1 and C_2. In $\mathbb{R}^{3,1}$ these spheres are characterized by $\{\Gamma(\boldsymbol{c}_1) \cap \Gamma(\boldsymbol{c}_2)\}$.* □

We complete this section with few examples which make use of Laguerre transformations and isotropic hypersurfaces.

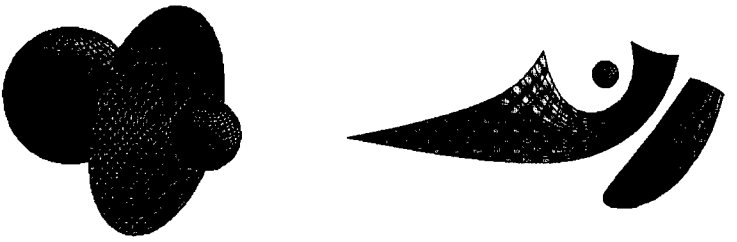

Fig. 3. Bisector of 2 spheres, resp. of sphere and canal surface.

Example 3. *Using the previous proposition and Example 2, implicit and parametric representation of cyclides C can be derived easily. With a Laguerre transformation τ, the corresponding pe circle can be mapped to a simple normal form $\underline{x}_3 = \underline{x}_4 = \underline{x}_1^2 + \underline{x}_2^2 - \underline{x}_0^2 = 0$ of a image cyclide $\tilde{C}$. Its isotropic hypersurface reads in implicit form as*

$$\Gamma(\tilde{c}) : (\underline{x}_0^2 + \underline{x}_1^2 + \underline{x}_2^2 + \underline{x}_3^2 - \underline{x}_4^2)^2 - 4\underline{x}_0^2(\underline{x}_1^2 + \underline{x}_2^2) = 0,$$

and in parametric form as

$$(\underline{x}_0(u,v,w), \underline{x}_1(u,v,w), \underline{x}_2(u,v,w), \underline{x}_3(u,v,w), \underline{x}_4(u,v,w)) =$$
$$([1-w][1+v^2] + w[1-u^2], [1-w][1-v^2], 2[1-w]v, 2wu, -w[1+u^2]).$$

The implicit and parametric representation of the original cyclide C can be obtained from $\{\tau^{-1}(\Gamma(\tilde{c}))\} \cap \mathbb{R}^3$. The intersection procedure is straightforward, since τ is a linear mapping. In the parametric case, the parameter w can be eliminated easily, because it occurs linearly in the parameter representation.

Example 4. *Consider two spheres S_1, S_2 specified by points $\boldsymbol{s}_1, \boldsymbol{s}_2 \in \mathbb{R}^{3,1}$. The intersection $\Gamma(\boldsymbol{s}_1) \cap \Gamma(\boldsymbol{s}_2)$ of their isotropic hypersurfaces is contained in the hyperplane $H_{12} : \langle \boldsymbol{x} - (\boldsymbol{s}_1 + \boldsymbol{s}_2)/2, \boldsymbol{s}_2 - \boldsymbol{s}_1 \rangle_{pe} = 0$. Thus, the bisector of S_1 and S_2 is the orthogonal projection of $H_{12} \cap \Gamma(\boldsymbol{s}_1)$ onto $\mathbb{R}^3$. Since $\Gamma(\boldsymbol{s}_1)$ is a hypercone, the bisector surface is a quadric surface. Fig. 3 shows two spheres and a part of their bisector surface (hyperboloid of two sheets).*

Example 5. *A similar technique allows the computation of the bisector of a sphere S and a canal surface C (specified by $\boldsymbol{s}$ and $\boldsymbol{c}(t) \in \mathbb{R}^{3,1}$). Now, $H_{12}(t) : \langle \boldsymbol{x} - (\boldsymbol{s} + \boldsymbol{c}(t))/2, \boldsymbol{c}(t) - \boldsymbol{s} \rangle_{pe} = 0$ depends on t. The bisector surface is obtained by the orthogonal projection of $H_{12} \cap \Gamma(\boldsymbol{c})$ onto $\mathbb{R}^3$. For a rational canal surface, $\Gamma(\boldsymbol{c})$ is a rational ruled hypersurface with parameter representation $\boldsymbol{g}(t,u,v)$ in $\mathbb{R}^{3,1}$ which is linear in v. After the intersection and projection operation, we obtain a rational bisector surface $\boldsymbol{b}(t,u)$. Fig. 3 depicts the bisector $\boldsymbol{b}(t,u)$ of a sphere and a canal surface $\boldsymbol{c}(t,u)$ with cubic spine curve and rational parametric degree (7,2). $\boldsymbol{b}(t,u)$ has parametric degree (10,2).*

Rational bisectors of spheres and PN surfaces are studied in [3]. Further applications of the concept of isotropic hypersurfaces can be found in [8] (tangent plane property) and [12] (offset property).

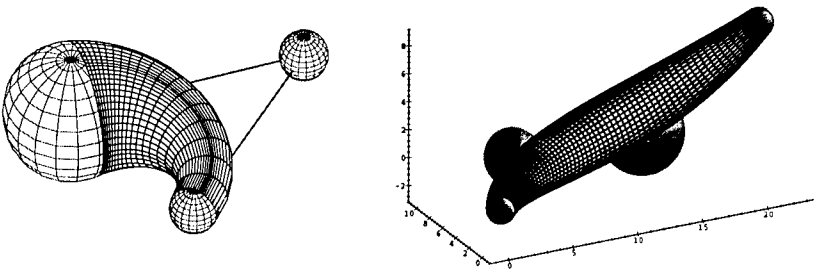

Fig. 4. Cyclide and cubic canal surface with control spheres.

§4. Control Sphere Representation

Consider a Bézier curve

$$\boldsymbol{x}(t) = \sum_{k=0}^{n} \boldsymbol{s}_k B_k^n(t) \tag{6}$$

of degree n in the cyclographic model with control points $\boldsymbol{s}_k \in \mathbb{R}^{3,1}$. They correspond to control spheres of the canal surface C described by $\boldsymbol{x}(t)$. Well-known properties of the Bernstein-Bézier technique can be applied directly to the Laguerre geometric approach (this idea was introduced in [12]):

Proposition 3.

1) *The de Casteljau algorithm enables a stable computation of the moving spheres of a canal surface and can be used to subdivide it into two parts.*
2) *The control spheres S_0 and S_1 (S_n and S_{n-1}) generate the tangent cone of the canal surface at $t = 0$ ($t = 1$).*
3) *A (rational) canal surface (with positive weights) lies in the convex hull of its control spheres.*

The control structure is useful from the designers point of view because the influence of moving the control spheres or changing their radius or weights is analogous to the well-known curve case. For example, Fig. 5 views the influence of modifying one weight of a canal surface with cubic spine curve: The weight β_1 is increased from 1 (left) to 10 (right). All other weights satisfy $\beta_i = 1$.

We have seen some advantages of using the control sphere representation of canal surfaces. However, often it is necessary to know a (rational) tensor-product representation. Therefore, one has to analyze the correlation between control spheres and classical control points of a canal surface. For the cyclide case there exists a simple geometric relation, which is described in [8]. In the case of an arbitrary canal surface, the problem was solved by Pottmann and Peternell [11]. They proved the surprising result that any canal surface with rational spine curve $\boldsymbol{m}(t)$ and rational radius function $r(t)$ is rational. Furthermore, they proved that the problem of finding the rational tensor-product representation can be reduced to the problem of finding two rational

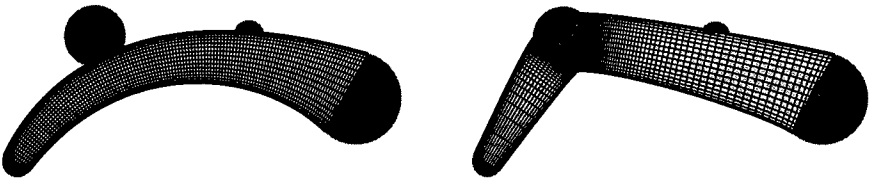

Fig. 5. Influence of different weights.

functions $\rho_1(t)$ and $\rho_2(t)$ which satisfy

$$\rho_1^2 + \rho_2^2 = \rho := \dot{m}_1^2 + \dot{m}_2^2 + \dot{m}_3^2 - \dot{r}^2. \tag{7}$$

Although the existence of solutions of (7) can be proved via factorization over the complex field, it is not trivial to find the (non-unique) solutions. There are two different options to perform the conversion from control spheres to control points:

1) Use arbitrary rational curves $\boldsymbol{x}(t) \in \mathbb{R}^{3,1}$ to describe canal surfaces. Then it is impossible to solve (7) exactly and numerical methods are required to compute the control points from the control spheres of the dedicated canal surface.
2) Use rational curves $\boldsymbol{x}(t) \in \mathbb{R}^{3,1}$ which have the property that $\rho(t)$ is a square in the polynomial ring $\mathbb{R}[t]$. Then an exact conversion from control spheres to control points can be realized using the algorithm of Pottmann and Peternell [11].

In this paper we will follow the second option. It results in the concept of Minkowski Pythagorean Hodograph curves.

§5. Minkowski Pythagorean Hodograph Curves in $\mathbb{R}^{3,1}$

Planar and spatial Pythagorean hodograph curves have been introduced by Farouki and Sakkalis [4,5]. Recently Moon [9] has generalized this class of curves and investigated the Minkowski Pythagorean hodograph (MPH) curves of $\mathbb{R}^{2,1}$. Here we need a further generalization: the MPH curves of $\mathbb{R}^{3,1}$:

Definition 2. *A polynomial (rational) curve* $\boldsymbol{x}(t) = (x_1(t), x_2(t), x_3(t), x_4(t))$ *in* $\mathbb{R}^{3,1}$ *is a* Minkowski Pythagorean hodograph *(MPH) curve if there exists a real polynomial (rational function)* $\sigma(t)$ *which satisfies*

$$\dot{x}_1^2(t) + \dot{x}_2^2(t) + \dot{x}_3^2(t) - \dot{x}_4^2(t) = \sigma^2(t). \tag{8}$$

As described before, for canal surfaces described via MPH curves of $\mathbb{R}^{3,1}$, an exact conversion from control spheres to control points can be realized. We now present some additional important properties of MPH curves.

Proposition 4.

1) *The tangent vector of a MPH curve is hyperbolic except a finite number of parabolic tangent vectors, i.e., the corresponding canal surface is always real.*
2) *The MPH property is invariant under Laguerre transformations.*
3) *PH space curves are exactly those MPH curves, which hold* $x_4 = 0$

Pe circles are examples for rational MPH curves of degree 2. In order to create polynomial MPH curves, equation (8) could be solved in a polynomial ring $\mathbb{R}[t]$. A possible solution (determined via stereographic projection) is

$$\begin{aligned}&(\dot{x}_1(t),\ \dot{x}_2(t),\ \dot{x}_3(t),\ \dot{x}_4(t),\ \sigma(t)) = \\ &(2u_0u_1,\ 2u_0u_2,\ -u_0^2+u_1^2+u_2^2-u_3^2,\ 2u_0u_3,\ u_0^2+u_1^2+u_2^2-u_3^2).\end{aligned} \tag{9}$$

The polynomials $\boldsymbol{u}(t) := (u_0(t), u_1(t), u_2(t), u_3(t))$ of degree n are mapped via (9) to polynomials of degree $2n$. Taking account of $x_i(t) = \int \dot{x}_i(t)\ dt + C$ with $i = 1, \ldots, 4$, we obtain a polynomial MPH curve of degree $2n+1$. Due to space limitations, we postpone a more detailed description. However, the basic principles of the analytic construction are the same as for MPH curves of $\mathbb{R}^{2,1}$, which are inspected by Moon [9] in detail.

An alternative approach is to construct MPH curves as Laguerre images of PH curves. For example, one could make use of well-known properties on spatial PH cubics [5,6,14] for building MPH cubics. Consider a cubic MPH Bézier curve $\boldsymbol{x}(t)$ with control points $\boldsymbol{b}_0, \boldsymbol{b}_1, \boldsymbol{b}_2, \boldsymbol{b}_3 \in \mathbb{R}^{3,1}$. $\boldsymbol{b}_0$ and $\boldsymbol{b}_1$ resp. $\boldsymbol{b}_2$ and $\boldsymbol{b}_3$ define two hyperbolic tangent vectors $\boldsymbol{t}_1$ and $\boldsymbol{t}_2$, which span a three-dimensional plane Π^3. If there exits a Laguerre transformation τ with $\tau(\Pi^3) = \mathbb{R}^3$, then $\boldsymbol{x}(t) = \tau^{-1}(\boldsymbol{y}(t))$ is a Laguerre image of a (spatial) PH cubic $\boldsymbol{y}(t) \in \mathbb{R}^3$ (that fact comes from properties 2) and 3) of proposition 4 in combination with the convex hull property of Bézier curves).

Proposition 5. *Consider a hyperplane* $\Pi^3 \subset \mathbb{R}^{3,1}$ *spanned by two skew hyperbolic lines* t_1 *and* t_2. *There exists a Laguerre transformation* τ *with* $\tau(\Pi^3) = \mathbb{R}^3$ *iff all lines joining* t_1 *and* t_2 *are hyperbolic.*

Proof: All straight lines in $\mathbb{R}^3$ are hyperbolic. Because of Corollary 2, it is necessary for the existence of τ, that any line of the linear congruence $t_1 \star t_2$ is hyperbolic, too. The sufficiency is proved by construction: With a pe rotation τ_1 one hyperbolic line t_1 can be mapped to $\mathbb{R}^3$. $\tau_1(t_1)$ and the point $\boldsymbol{p} := \tau_1(t_2) \cap \mathbb{R}^3$ span a 2-dimensional plane $\Pi^2 \subset \mathbb{R}^3$. An appropriate Euclidean motion τ_2 maps Π^2 onto the x_2, x_3-plane. Let $\boldsymbol{q} = (q_1, 0, 0, q_4)$ be the intersection point of $\tau_2 \circ \tau_1(t_2)$ with the x_1, x_4-plane. Case 1) $|q_1| < |q_4|$: the pe rotation (5) with $\alpha = \operatorname{arctanh}(-q_1/q_4)$ maps $\tau_2 \circ \tau_1(\Pi^3)$ onto the hyperplane $x_1 = 0$. Since it contains elliptic lines, this contradicts the assumption that $t_1 \star t_2$ is hyperbolic. Case 2) $|q_1| = |q_4|$: $\tau_2 \circ \tau_1(\Pi^3)$ is the hyperplane $x_1 = x_4$. Since it contains parabolic lines, we also get a contradiction. It remains to consider Case 3) $|q_1| > |q_4|$: the pe rotation (5) with $\alpha = \operatorname{arctanh}(-q_4/q_1)$ maps $\tau_2 \circ \tau_1(\Pi^3)$ onto $\mathbb{R}^3$. □

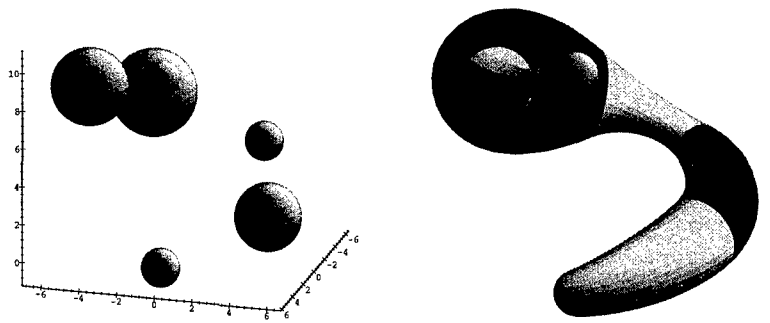

Fig. 6. Interpolation of spheres with cyclide spline.

§6. Interpolation with Canal Surfaces

Finally we briefly discuss simple interpolation problems concerning canal surfaces. The construction of canal surfaces which interpolate given spheres or tangent cones is reduced in the cyclographic model to finding an interpolating curve in $\mathbb{R}^{3,1}$. Therefore, standard algorithms can be generalized from $\mathbb{R}^3$ to $\mathbb{R}^{3,1}$ in order to solve the problem. Indeed, one has to take into account that these methods could generate curves with elliptic tangent vectors, which does not comply with real canal surfaces! This problem can be avoided using algorithms which deal with MPH curves.

Example 6. $n+1$ spheres P_i $(i = 0, \ldots, n)$ can be interpolated with a G^1-continuous cyclide spline (Fig. 6). Each piece is characterized by a pe circle segment with control points $\boldsymbol{b}_{k,i} \in \mathbb{R}^{3,1}$ and weights $\beta_{k,i} \in \mathbb{R}$, $k = 0, 1, 2$. Per given tangent vector $\boldsymbol{t}_{i-1}$ at $\boldsymbol{p}_{i-1}$ the segment is determined uniquely. Thus with any starting vector $\boldsymbol{t}_0$, the pe circular spline curve can be produced successively. To perform the computation, one can generalize an ordinary circular spline algorithm. The formulas (10) are cited from [13], just replacing the Euclidean metric by the pe metric:

$$\begin{aligned} \boldsymbol{b}_{0,i} &= \boldsymbol{p}_{i-1}, \quad \boldsymbol{b}_{1,i} = \boldsymbol{p}_{i-1} + \frac{\|\Delta \boldsymbol{p}_i\|_{pe}^2}{2\langle \Delta \boldsymbol{p}_i, \boldsymbol{t}_{i-1}\rangle_{pe}}, \quad \boldsymbol{b}_{2,i} = \boldsymbol{p}_i, \\ \beta_{0,i} &= 1, \quad \beta_{1,i} = \frac{\langle \Delta \boldsymbol{p}_i, \boldsymbol{t}_{i-1}\rangle_{pe}}{\|\Delta \boldsymbol{p}_i\|_{pe}\|\boldsymbol{t}_{i-1}\|_{pe}}, \quad \beta_{2,i} = 1. \end{aligned} \tag{10}$$

The only condition on the input data is $\|\Delta \boldsymbol{p}_i\|_{pe} := \|\boldsymbol{p}_i - \boldsymbol{p}_{i-1}\| > 0$, i.e., the spheres P_{i-1} and P_i cannot lie inside each other.

Example 7. A piecewise Hermite interpolant can be realized with a cubic MPH canal surface. Consider two spheres P_{i-1}, P_i (specified by points $\boldsymbol{p}_{i-1}$, $\boldsymbol{p}_i$ in $\mathbb{R}^{3,1}$) and tangent cones T_{i-1}, T_i (described as hyperbolic lines $\boldsymbol{t}_{i-1}$,$\boldsymbol{t}_i \in \mathbb{R}^{3,1}$ spanning a hyperplane $\Pi^3 \subset \mathbb{R}^{3,1}$). If this input data satisfy the condition of Proposition 5, then there exists a Laguerre transformation

τ which maps Π^3 to $\mathbb{R}^3$, and a well-known Hermite interpolation algorithm [6,14] produces a cubic PH Hermite interpolant $\boldsymbol{c}(t) \in \mathbb{R}^3$. Its Laguerre image $\tau^{-1}(\boldsymbol{c}(t))$ is a cubic MPH curve and interpolates the original input data.

References

1. Boehm, W., Circles of curvature for curves in space, Comput. Aided Geom. Design **16** (1999), 633–638.
2. Cecil, T. E., *Lie Sphere Geometry*, Springer, New York, 1992.
3. Elber, G., and M. S. Kim, Computing rational bisectors, IEEE Computer Graphics & Applications **19** (1999), 76–81.
4. Farouki, R. T., and T. Sakkalis, Pythagorean Hodographs, IBM J. Res. Dev. **34** (1990), 736–752.
5. Farouki, R. T., and T. Sakkalis, Pythagorean-hodograph space curves, Advances in Computational Mathematics **2** (1994), 41–66.
6. Jüttler, B., and C. Mäurer, Cubic Pythagorean hodograph spline curves and applications to sweep surface modeling, Computer-Aided Design **31** (1999), 73–83.
7. Krasauskas, R., and C. Mäurer, Studying cyclides with Laguerre geometry, Comput. Aided Geom. Design, to appear.
8. Mäurer, C., and R. Krasauskas, Joining cyclide patches along quartic boundary curves, in *Mathematical Methods for Curves and Surfaces II*, M. Dæhlen, T. Lyche, and L. L. Schumaker (eds.), Vanderbilt University Press, Nashville, 1998, 359–366.
9. Moon, H. P., Minkowski Pythagorean hodographs, Comput. Aided Geom. Design **16** (1999), 739–753.
10. Paluszny, M., and W. Boehm, General cyclides, Comput. Aided Geom. Design **15** (1998), 699–710.
11. Peternell, M., and H. Pottmann, Computing rational parametrizations of canal surfaces, Journal of Symbolic Comutation **23** (1997), 255–266.
12. Pottmann, H., and M. Peternell, Applications of Laguerre geometry in CAGD, Comput. Aided Geom. Design **15** (1998), 165–186.
13. Seemann, G., Kreissplines und Schraubliniensplines: Interpolation und Approximation durch Raumkurven mit konstanten Invarianten, PhD-thesis, TU Darmstadt, 1995.
14. Wagner, M., and B. Ravani, Curves with rational Frenet frame motion, Comput. Aided Geom. Design **15** (1997), 79–101.

Christoph Mäurer
TWT-GmbH
Finkenstr. 16
70794 Filderstadt, Germany
fa-twt.christoph.maeurer@daimlerchrysler.com